Three-body interactions with cold polar molecules

H. P. BÜCHLER*, A. MICHELI AND P. ZOLLER

Institute for Theoretical Physics, University of Innsbruck, 6020 Innsbruck, Austria
Institute for Quantum Optics and Quantum Information, 6020 Innsbruck, Austria
***e-mail: hanspeter.buechler@uibk.ac.at**

Published online: 22 July 2007; doi:10.1038/nphys678

Fundamental interactions between particles, such as the Coulomb law, involve pairs of particles, and our understanding of the plethora of phenomena in condensed-matter physics rests on models involving effective two-body interactions. On the other hand, exotic quantum phases, such as topological phases or spin liquids, are often identified as ground states of hamiltonians with three- or more-body terms. Although the study of these phases and the properties of their excitations is currently one of the most exciting developments in theoretical condensed-matter physics, it is difficult to identify real physical systems exhibiting such properties. Here, we show that polar molecules in optical lattices driven by microwave fields naturally give rise to Hubbard models with strong nearest-neighbour three-body interactions, whereas the two-body terms can be tuned with external fields. This may open a new route for an experimental study of exotic quantum phases with quantum degenerate molecular gases.

The many-body hamiltonians underlying condensed-matter physics are derived within an effective low-energy theory, obtained by integrating out the high-energy excitations. In general, this gives rise to interaction terms

$$V_{\mathrm{eff}}(\{\mathbf{r}_i\}) = \sum_{i<j} V(\mathbf{r}_i - \mathbf{r}_j) + \sum_{i<j<k} W(\mathbf{r}_i, \mathbf{r}_j, \mathbf{r}_k) + \cdots \qquad (1)$$

where $V(\mathbf{r})$ describes the two-particle interaction depending only on the separation between the particles. The second term, $W(\mathbf{r}_i, \mathbf{r}_j, \mathbf{r}_k)$, is the three-body interaction, which depends on the distance and orientation of three particles, and vanishes if one particle is far from the other two. The ellipsis denotes possible higher many-body terms. Although for helium atoms in the context of superfluidity the two-particle interaction dominates and determines the ground-state properties with the three-body interactions providing small corrections[1], model hamiltonians with strong three-body interactions have attracted a lot of interest in the search for microscopic hamiltonians exhibiting exotic ground-state properties. Well-known examples are the fractional quantum Hall states described by the pfaffian wavefunctions, which appear as ground states of a hamiltonian with three-body interaction[2–4]. These topological phases admit anyonic excitations with non-abelian braiding statistics. Also of special interest are spin systems and bosonic hamiltonians with complex many-body interactions, such as the ring exchange model, which are expected to give rise to exotic phases[5–8]. Three-body interactions are also an essential ingredient for systems with a low-energy degeneracy characterized by string nets[9,10], which play an important role in models for non-abelian topological phases. The main challenge is then to identify experimentally accessible systems, where the two-particle interaction $V(\mathbf{r})$ can be controlled, independently of the three-body interaction $W(\mathbf{r}_i, \mathbf{r}_j, \mathbf{r}_k)$.

Here, we analyse the effective interaction potential in a many-body system of polar molecules. Recently, systems of polar molecules in the rovibrational ground state have attracted a lot of interest owing to their rich internal structure and the presence of large permanent dipole moments, which give rise to dipole–dipole interactions and offer the possibility to tune the interaction with static electric fields and microwave fields[11–16]. Techniques for trapping and cooling polar molecules with the goal to create quantum degenerate ground-state molecules are currently being developed in several laboratories[17–24]. We show below that for an appropriate choice of static electric and microwave fields, the effective interaction reduces to the form as in equation (1) with tunable two-body and three-body interactions.

In particular, for polar molecules moving in an optical lattice we obtain the Hubbard model

$$H = -J \sum_{\langle ij \rangle} b_i^\dagger b_j + \sum_{i \neq j} \frac{U_{ij}}{2} n_i n_j + \sum_{i \neq j \neq k} \frac{W_{ijk}}{6} n_i n_j n_k . \qquad (2)$$

Here, b_i ($b_i^\dagger$) are destruction (creation) operators for a molecule on lattice site i, satisfying canonical commutation (anti-commutation) relations for bosonic (fermionic) molecules, and a hard-core on-site repulsion is implied for bosons. The first term in equation (2) is a hopping term (kinetic energy), whereas the last two terms describe two-body and three-body interaction terms ($n_i = b_i^\dagger b_i$). The different strengths of the three-body interaction terms are shown in Fig. 1. We emphasize that our derivation of the Hubbard model, equation (2), resulting in strong and tunable two and three-body interactions, will be based directly on the effective many-particle potential, equation (1). This is in contrast to the common approach to derive effective many-body terms from Hubbard models involving two-body interactions, which are obtained in a $J \ll U$ perturbation theory, and are thus necessarily small[25]. The main part of this work is concerned with the microscopic derivation of the hamiltonian in equation (2), and the tunability of the parameters by external fields. As an illustration, we analyse the simplest possible case of a one-dimensional Bose–Hubbard

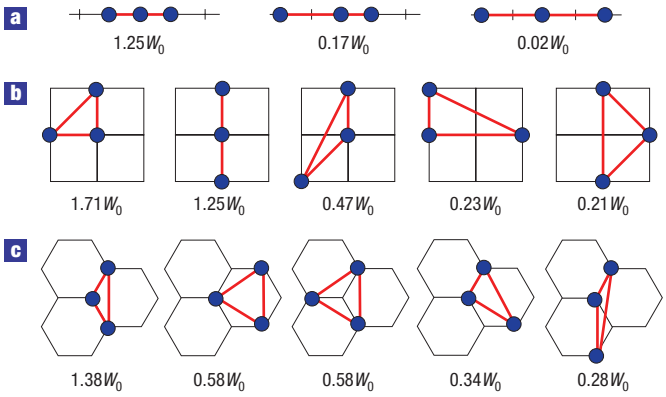

Figure 1 Three-body interaction terms. Strengths of the dominant three-body interactions W_{ijk} appearing in the Hubbard model for different lattice geometries. **a**, One-dimensional set-up. **b**, Two-dimensional square lattice. **c**, Two-dimensional honey-comb lattice. The characteristic energy scale $W_0 = \gamma_2 D R_0^6 / a^6$ is discussed following equation (6).

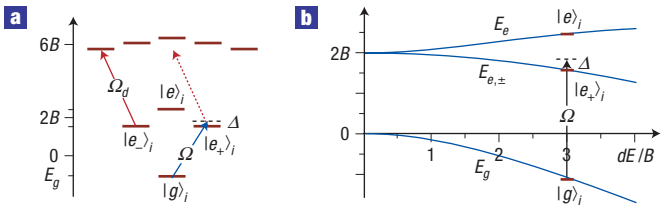

Figure 2 Spectrum of a polar molecule. a, Level structure for $Ed/B = 3$: the circularly polarized microwave field couples the ground state $|g\rangle$ with the excited state $|e_+\rangle$ with Rabi frequency $\Omega/\hbar$ and detuning Δ. The excited state $|e_+\rangle$ is characterized by a finite angular momentum $J_z|e_+\rangle = |e_+\rangle$. Applying a second microwave field with opposite polarization (red arrow) allows us to lift the degeneracy in the first excited manifold by resonantly coupling the state $|e_-\rangle$ to the next manifold. **b**, Internal excitation energies for a single polar molecule in a static electric field $\mathbf{E} = E\mathbf{e}_z$.

model with a dominant three-body interaction, and derive the phase diagram using bosonization techniques.

EFFECTIVE INTERACTION POTENTIAL

We start with deriving the effective low-energy interaction potential of the form of equation (1) for polar molecules interacting via dipole–dipole interaction. The formal derivation is based on dressing low-lying rotational states with external static electric fields and near-resonant microwave fields, which allows us to map the hamiltonian onto an interacting spin-1/2 system. In the spirit of the Born–Oppenheimer approximation, we will interpret the interaction energy in a given dressed state and for a given spatial configuration $\{\mathbf{r}_i\}$ as the effective interaction potential V_{eff}.

The internal low-energy structure of polar molecules with a closed-shell electronic structure $^1\Sigma$ is given by the rotational degree of freedom, and its low-energy excitations are well described by the rigid-rotor hamiltonian

$$H_{\mathrm{rot}}^{(i)} = B\mathbf{J}_i^2 - \mathbf{d}_i\mathbf{E}(t),$$

where B is the rotational constant and $\mathbf{J}_i$ is the dimensionless angular momentum operator. The last term accounts for an external electric field with $\mathbf{d}_i$, the dipole operator.

We focus on a set-up with a static electric field $\mathbf{E} = E\mathbf{e}_z$ along the z axis, see Fig. 2, where the two states $|g\rangle_i$ and $|e_+\rangle_i$ with energies E_g and $E_{e,\pm}$ are coupled by a circularly polarized microwave field propagating along the z axis. The microwave transition is characterized by the detuning Δ and the Rabi frequency $\Omega/\hbar$. The internal structure of a single polar molecule reduces to a two-level system and is described as a spin-1/2 particle via the identification of the state $|g\rangle_i$ ($|e_+\rangle_i$) as eigenstates of the spin operator S_i^z with positive (negative) eigenvalue. In the rotating frame and applying the rotating-wave approximation, the hamiltonian describing the internal dynamics of the polar molecule reduces to

$$H_0^{(i)} = \frac{1}{2}\begin{pmatrix} \Delta & \Omega \\ \Omega & -\Delta \end{pmatrix} = \mathbf{h}\mathbf{S}_i,$$

with the effective magnetic field $\mathbf{h} = (\Omega, 0, \Delta)$ and the spin operator $\mathbf{S}_i = (S_i^x, S_i^y, S_i^z)$. The eigenstates of this hamiltonian are denoted as $|+\rangle_i = \alpha|g\rangle_i + \beta|e_+\rangle_i$ and $|-\rangle_i = -\beta|g\rangle_i + \alpha|e_+\rangle_i$ with energies $\pm\sqrt{\Delta^2 + \Omega^2}/2$.

The interaction between the polar molecules is determined by the dipole–dipole interaction

$$V_{\mathrm{d-d}}(\mathbf{r}_{ij}) = \frac{\mathbf{d}_i\mathbf{d}_j}{|\mathbf{r}_{ij}|^3} - \frac{3(\mathbf{r}_{ij}\mathbf{d}_i)(\mathbf{r}_{ij}\mathbf{d}_j)}{|\mathbf{r}_{ij}|^5},$$

where $\mathbf{r}_{ij} = \mathbf{r}_i - \mathbf{r}_j$ is the separation between the particles. In the interesting regime with $|\mathbf{r}_{ij}| \gg (D/B)^{1/3}$, we can map the dipole–dipole interaction restricted to the states $|e_+\rangle_i$ and $|g\rangle_i$ onto an effective spin-interaction hamiltonian. Using the rotating-wave approximation, the interaction hamiltonian within the rotating frame reduces to $H_{\mathrm{d}} = H_{\mathrm{d}}^{\mathrm{int}} + H_{\mathrm{d}}^{\mathrm{shift}}$. The first term describes an effective spin–spin interaction

$$H_{\mathrm{d}}^{\mathrm{int}} = -\frac{1}{2}\sum_{i\neq j} D\nu(\mathbf{r}_{ij})\left[S_i^x S_j^x + S_i^y S_j^y - \eta_-^2 S_i^z S_j^z\right],$$

where D denotes the coupling strength between the two states $D = |\langle g|\mathbf{d}_i|e_+\rangle|^2$, whereas $\eta_\pm = \eta_g \pm \eta_e$ is determined by the induced dipole moments $\eta_g = \partial_E E_g/\sqrt{D}$ and $\eta_e = \partial_E E_{e,+}/\sqrt{D}$. The anisotropic behaviour of the dipole–dipole interaction is accounted for by $\nu(\mathbf{r}) = (1 - 3\cos^2\theta)/r^3$, where θ is the angle between $\mathbf{r}$ and the z axis. In addition, the asymmetry of the induced dipole moments gives rise to a position-dependent renormalization of the effective magnetic field and an energy shift

$$H_{\mathrm{d}}^{\mathrm{shift}} = \frac{1}{2}\sum_{i\neq j} D\nu(\mathbf{r}_{ij})\left[\frac{\eta_-\eta_+}{2} S_i^z + \frac{\eta_+^2}{4}\right].$$

Note, that the dipole–dipole interaction can also induce transitions between the states $|e_-\rangle$ and $|e_+\rangle$ if the two states are degenerate. In the following, we assume that the degeneracy of the states $|e_-\rangle$ and $|e_+\rangle$ is lifted by a further microwave field coupling the state $|e_-\rangle$ near-resonantly to the next state manifold, see Fig. 2; the analysis for the degenerate situation is presented in the Methods section.

Next, we are interested in the effective interaction between the polar molecules with each molecule prepared in the state $|+\rangle_i$. Within the Born–Oppenheimer approximation, we determine the eigenenergies of the internal hamiltonian $\sum_i H_0^{(i)} + H_d$ for fixed particle positions $\{\mathbf{r}_i\}$ and obtain the energy shift of the state adiabatically connected to the state $|G\rangle = \Pi_i|+\rangle_i$ of the non-interacting system. This energy shift is driven by the dipole–dipole interaction H_{d} and strongly depends on

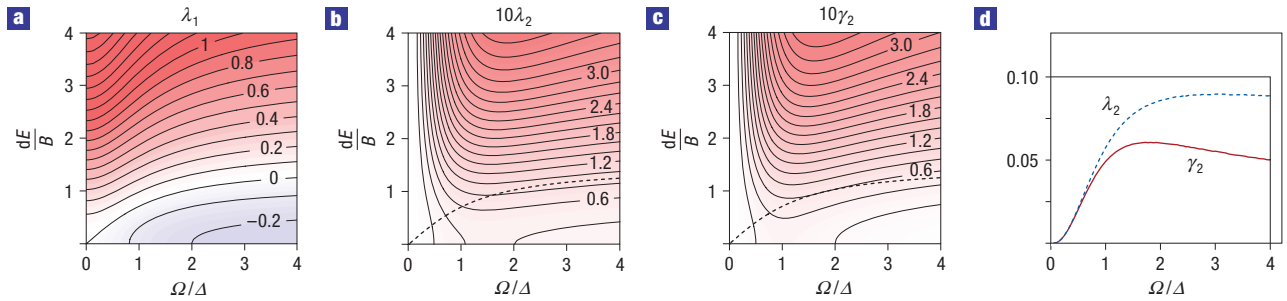

Figure 3 Parameters of the effective interaction potential. a–c, Strength of the interaction parameters λ_1, λ_2 and γ_2 as a function of the external fields Ed/B and Ω/Δ. The leading dipole–dipole interaction vanishes for $\lambda_1 = 0$ (dashed line in **b**,**c**), and the second-order contributions dominate the interaction. **d**, Strength of λ_2 (dashed line) and γ_2 (solid line) along the line in parameter space with $\lambda_1 = 0$.

the positions of the particles $\{\mathbf{r}_i\}$ and therefore describes the effective interaction $V_{\rm eff}(\{\mathbf{r}_i\})$. This energy shift in the current situation can be calculated within perturbation theory, see the Methods section. The small parameter controlling the perturbative expansion is $D/(a^3|\mathbf{h}|) = (R_0/a)^3$, where a is the characteristic length scale of the interparticle separation and the length scale $R_0 = (D/\sqrt{\Delta^2+\Omega^2})^{1/3}$.

The effective interaction potential $V_{\rm eff}$ reduces to the form in equation (1) with the two-particle interaction potential

$$V(\mathbf{r}) = \lambda_1 D v(\mathbf{r}) + \lambda_2 D R_0^3 [v(\mathbf{r})]^2, \tag{3}$$

and the three-body interaction

$$W(\mathbf{r}_1,\mathbf{r}_2,\mathbf{r}_3) = \gamma_2 R_0^3 D[v(\mathbf{r}_{12})v(\mathbf{r}_{13}) + v(\mathbf{r}_{12})v(\mathbf{r}_{23}) + v(\mathbf{r}_{13})v(\mathbf{r}_{23})]. \tag{4}$$

The dimensionless coupling parameters λ_1, λ_2 and γ_2 are presented in the Methods section. These parameters can be tuned via the strength of the electric field Ed/B and the ratio between the Rabi frequency and the detuning Ω/Δ see Fig. 3. Of special interest are the values of the external fields, where $\lambda_1 = 0$, that is, the leading two-particle interaction vanishes. Then, the interaction is dominated by the second-order contribution with λ_2 and γ_2, which includes the three-body interaction, see Fig. 3d, whereas small deviation away from the line $\lambda_1 = 0$ allows us to change the character of the two-particle interaction.

The perturbative expansion requires that the interparticle distance is larger than the length scale R_0, and limits the validity of the effective interaction $V_{\rm eff}(\{\mathbf{r}_i\})$ to a regime with $|\mathbf{r}_i - \mathbf{r}_j| > R_0$. Note that within this regime, the Born–Oppenheimer approximation is also valid as the different dressed manifolds are separated by the high-energy scale Δ suppressing diabatic transitions. Here, we prevent particles from approaching each other on shorter distances, $|\mathbf{r}_i - \mathbf{r}_j| < R_0$, by focusing on set-ups where the combination of interparticle potential for $|\mathbf{r}_i - \mathbf{r}_j| > R_0$ and the transverse trapping potential produces a strong repulsive barrier. For sufficiently strong barrier height, thermal activation across the barrier and quantum mechanical tunnelling through the barrier are then suppressed, and the particles are confined in parameter space to the region $|\mathbf{r}_i - \mathbf{r}_j| > R_0$. A set-up providing such a barrier is obtained by confining the particles into two dimensions by a strong transverse trapping potential along the z axis with transverse trapping frequency $\omega_\perp = \hbar/ma_\perp^2$ as provided, for example, by an optical lattice. The condition for an efficient barrier in this two-dimensional set-up has been recently worked out for polarized molecules with leading dipole–dipole interaction[26,27]. However, the analysis can be generalized to the current situation with the interaction potential $V_{\rm eff}(\{\mathbf{r}_i\})$ if the two-particle potential $V(\mathbf{r})$ is sufficiently repulsive, that is, $\lambda_1 \gtrsim -\lambda_2(R_0/a)^3$. For $\hbar\omega_\perp > D/R_0^3$, an estimate of the rate for two particles to penetrate the barrier up to a distance $|\mathbf{r}_i - \mathbf{r}_j| < R_0$ is provided by $\Gamma \sim (\hbar/ma^2)\exp(-2S_{\rm E}/\hbar)$ with the semiclassical action $S_{\rm E}/\hbar \sim \sqrt{Dm/R_0\hbar^2}$. This exponential suppression confines particles in parameter space to the region $|\mathbf{r}_i - \mathbf{r}_j| > R_0$ for realistic parameters with polar molecules, see below.

The low-energy many-body theory now follows by combining the kinetic energy of the polar molecules with the effective interaction $V_{\rm eff}$ within the Born–Oppenheimer approximation and the external trapping potentials $V_{\rm T}$

$$H = \sum_i \frac{\mathbf{p}_i^2}{2m} + V_{\rm eff}(\{\mathbf{r}_i\}) + \sum_i V_{\rm T}(\mathbf{r}_i). \tag{5}$$

Note that the hamiltonian is independent of the statistics of the particles and therefore is valid for bosonic and fermionic polar molecules. In the strongly interacting regime, where the interaction energy dominates over the kinetic energy, it is expected that the ground state of the many-body system is determined by crystalline phases[27].

HUBBARD MODEL

Applying an optical lattice provides a periodic structure for the polar molecules described by the hamiltonian equation (5) and allows us to derive Hubbard models with unconventional and strong nearest-neighbour interactions. We focus on the above set-up, where the stability of the system is obtained by a strong transverse trapping potential. We describe the lattice structure with lattice spacing a by a set of vectors $\{\mathbf{R}_i\}$ accounting for the minima of the optical lattice; depending on the optical lattice, we can generate one-dimensional and two-dimensional systems. The mapping to the Hubbard model follows the standard procedure[28]. (1) Solving the single-particle problem in the presence of the optical lattice provides the Wannier functions $w(\mathbf{r})$ for the lowest Bloch band and determines the hopping energy J. The Wannier functions describe localized wavefunctions with characteristic size a_0. (2) We express the field operator ψ in terms of the Wannier functions in the lowest band $\psi^\dagger(\mathbf{r}) = \sum_i w(\mathbf{r} - \mathbf{R}_i)b_i^\dagger$, where $b_i^\dagger$ (b_i) is the creation (annihilation) operator at the lattice site $\mathbf{R}_i$. To simplify the discussion, we consider bosonic particles satisfying bosonic

Table 1 Parameters of the sine-Gordon term.

	u	β
$n=1/3$	Wa/π	$\sqrt{36\pi}$
$n=1/2$	$Wa/2$	$\sqrt{16\pi}$
$n=2/3$	Wa/π	$\sqrt{36\pi}$

commutation relations. Expressing the hamiltonian in equation (5) in second quantization and inserting the bosonic field operator ψ, maps the system to the Bose–Hubbard model. However, the on-site interaction, which is derived for cold atomic gases from the pseudopotential, requires a special discussion in the current situation. In the experimentally interesting regime, we have the following separation of the length scales: $a_0 \leq R_0 < a$. With the above discussion, that the parameter space of the system is confined to interparticle distances larger than R_0, this implies that if a particle is at site $\mathbf{R}_i$, the hopping rate for a second particle to tunnel to this site is strongly suppressed. As the initial system has no doubly occupied sites, a convenient way to express this conditional hopping is to describe the bosons as hard-core bosons. Consequently, no on-site interaction term is present, and we obtain the Bose–Hubbard model in equation (2). The interaction parameters U_{ij} and V_{ijk} derive from the effective interaction $V(\{\mathbf{r}_i\})$ and in the limit of well-localized Wannier functions ($a_0/a \ll 1$) reduce to $U_{ij} = V(\mathbf{R}_i - \mathbf{R}_j)$ and $W_{ijk} = W(\mathbf{R}_i, \mathbf{R}_j, \mathbf{R}_k)$. The decay of these interactions with interparticle separation takes the form

$$U_{ij} = U_0 \frac{a^3}{|\mathbf{R}_i - \mathbf{R}_j|^3} + U_1 \frac{a^6}{|\mathbf{R}_i - \mathbf{R}_j|^6},$$

$$W_{ijk} = W_0 \left[\frac{a^6}{|\mathbf{R}_i - \mathbf{R}_j|^3 |\mathbf{R}_i - \mathbf{R}_k|^3} + \text{perm} \right]. \qquad (6)$$

Here, $U_0 = \lambda_1 D/a^3$, $U_1 = \lambda_2 D R_0^3/a^6$ and $W_0 = \gamma_2 D R_0^3/a^6$ denote characteristic energy scales. The dominant contributions and strengths of the three-body terms in different lattice geometries are shown in Fig. 1.

In the following, we estimate these energy scales for LiCs with a permanent dipole moment $d = 6.3$ D. Assuming an optical lattice with lattice spacing $a \approx 500$ nm, the characteristic dimensionless parameter determining the ratio between the interaction energy ($E_{\text{int}} = D/a^3$) and the characteristic kinetic energy within the lattice ($E_{\text{kin}} = \hbar^2/ma^2$ proportional to the recoil energy) becomes $r_d = Dm/\hbar^2 a \approx 55$. The leading dipole–dipole interaction can give rise to very strong nearest-neighbour interactions with $U_0 \sim 55 E_{\text{kin}}$. On the other hand, by tuning the parameters via the external fields to $\lambda_1 = 0$, the characteristic energy scale for the three-body interaction becomes $W_0 \approx (R_0/a)^3 E_{\text{kin}}$. Then, controlling the hopping energy, J, via the strength of the optical lattice allows us to enter the regime with dominant three-body interactions.

THREE-BODY INTERACTIONS IN ONE DIMENSION

As an illustration, we study the one-dimensional system with leading three-body interaction. By tuning the external fields to a point with $U_1 = -U_0$, the hamiltonian takes the form

$$H = -J \sum_i \left[b_i^\dagger b_{i+1} + b_{i+1}^\dagger b_i \right] + W \sum_i n_{i-1} n_i n_{i+1}, \qquad (7)$$

where we have kept only the nearest-neighbour terms. The further interaction terms play a minor role in the following analysis. Using a Jordan–Wigner transformation allows us to map the hard-core bosons onto an interacting Fermi system, which can be studied using bosonization techniques[29,30]; the details of the calculation are presented in the Methods section. As a final result, we find that the low-energy hamiltonian is described by the sine-Gordon model for the particle densities $n = 1/3$, $n = 1/2$ and $n = 2/3$,

$$H = \frac{\hbar v}{2} \int \mathrm{d}x \left[K \Pi^2 + \frac{1}{K} (\partial_x \Phi)^2 \right] + u \int \mathrm{d}x \frac{1}{\pi^2 a^2} \cos(\beta \Phi). \qquad (8)$$

The parameters u and β for the sine term are given in Table 1. The renormalized Fermi velocity is $v = 2Ja \sin(\pi n)/\hbar K$, whereas the dimensionless Luttinger parameter takes the form $K = 1/\sqrt{1+\kappa}$ with

$$\kappa = \frac{W}{2J} \frac{2n}{\pi} \frac{3 - 2\cos(2\pi n) - \cos(4\pi n)}{\sin(\pi n)}.$$

The hamiltonian in equation (8) now allows for the derivation of the expected phases diagram.

For weak interactions, $W/2J < 1$, the three-body interaction shifts the hard-core bosons away from the Tonks gas limit ($K = 1$) into the correlated regime with $K < 1$. This regime is characterized by algebraic correlation functions; for example, the off-diagonal correlation between the bosons decays as $\langle b_i b_j^\dagger \rangle \sim |i - j|^{-1/2K}$, and the density–density correlation $\langle (n_i - n)(n_j - n) \rangle \sim \cos[2\pi n(i-j)]/|i-j|^{2K}$ (ref. 31). At three values of the density, $n = 2/3$, $n = 1/2$ and $n = 1/3$, the sine-Gordon term drives an instability towards a gapped phase, see Fig. 4. The critical value of K for this instability is given by $K = 8\pi/\beta^2$. In the following, we use this criterion to identify the instabilities towards three solid phases for $W/2J \sim 1$; the exact determination of the critical interaction strength requires an analysis beyond the scope of this paper. These solid phases are characterized by a broken translational symmetry, where the following observables allow us to distinguish the different ground states

$$\langle n_j \rangle \sim \cos\left[2\pi j n + \sqrt{4\pi}\, \Phi_l \right],$$

$$\langle b_j b_{j+1}^\dagger + b_j^\dagger b_{j+1} \rangle \sim \cos\left[(2\pi j + \pi) n + \sqrt{4\pi}\, \Phi_l \right], \qquad (9)$$

with Φ_l characterizing the different ground states. The first observable describes a density wave with wavevector $k = 2\pi n/a$

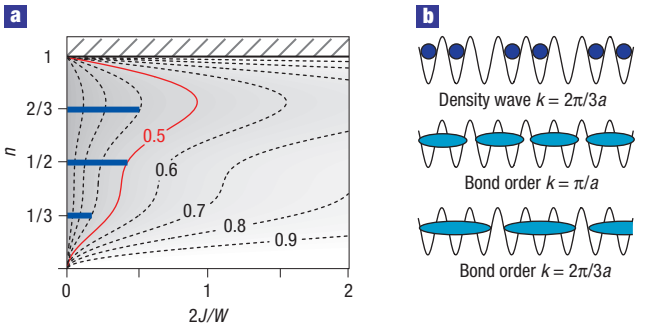

Figure 4 Phase diagram. a, $W/J - n$ phase diagram; the dashed contours correspond to constant values of K. The first instability at $n = 1/2$ appears for $K = 1/2$ (thin solid line), whereas the instabilities at $n = 1/3$ and $n = 2/3$ appear at lower values of K. Note that the interaction strength approaches $W/2J \approx 1$ at the position of the instabilities, and we expect the exact position of the instability to be strongly renormalized. **b**, Diagram of the three different solid orders characterizing the gapped phases: density order with wavevector $k = 2\pi/3a$, bond order with $k = \pi/a$ and bond order with wavevector $k = 2\pi/3a$.

present in conventional solids, whereas the second observable accounts for a bond order with wavevector $k=2\pi n/a$; see Fig. 4b for a diagram of the different orders appearing in the ground state.

At half filling, $n=1/2$, the instability towards a gapped phase appears for $K=1/2$. Within the gapped phase, the sine-Gordon term in equation (8) determines the long-distance behaviour, and the phase field, Φ, is predominantly pinned within a minimum of the $\cos(\sqrt{16\pi}\Phi)$ term. The minima take the form $\Phi_l=\pi(2l+1)/\sqrt{16\pi}$ and characterize the different ground states in the gapped phase. These ground states can be distinguished by the bond observable in equation (9). Therefore, we obtain a two-fold degenerate phase with a broken translational symmetry: the bond correlation function exhibits a long-range order at the wavevector $k=\pi/a$, whereas the density $\langle n_j\rangle$ remains uniform in this phase. The corresponding phase in spin systems is denoted as a spin-Peierls phase[30].

In turn, for the densities $n=1/3$ and $n=2/3$ the instability appears at lower values of K. The ground states of the gapped phase are then characterized by the minima of $\cos(\sqrt{36\pi}\Phi)$, which are given by $\Phi_l=\pi(2l+1)/\sqrt{36\pi}$. The different ground states can be distinguished by the density and bond observable providing a three-fold degenerate phase with a density wave and a bond order at the wavevector $k=2\pi/3$. The appearance of a density wave with $k=2\pi/3$ is a special property of the three-body interaction. It can be well understood for $n=2/3$ in the limit $W/2J\gg 1$: then the ground state takes the form $\Pi_i b^\dagger_{3i}b^\dagger_{3i+1}|0\rangle$ and describes a perfect density wave.

Within the above bosonization approach, the further interaction terms beyond the nearest-neighbour three-body interaction only provide a small renormalization of the coupling parameters in equation (8), and therefore play a minor role in the qualitative discussion of the instabilities. However, in the limit $W/2J\gg 1$ they become important and can give rise to further solid phases.

METHODS

ENERGY SHIFTS

The system is initially prepared into the eigenstate of the non-interacting system $|G\rangle=\Pi_i|+\rangle$ with $\Delta>0$ blue-detuned. Within first-order perturbation theory in the interaction hamiltonian $H_{\rm d}$, we obtain the energy shift

$$E^{(1)}(\{\mathbf{r}_i\})=\frac{1}{2}\Big[\big(\alpha^2\eta_g+\beta^2\eta_e\big)^2-\alpha^2\beta^2\Big]\sum_{i\neq j}D v(\mathbf{r}_{ij}).$$

Applying the Born–Oppenheimer approximation, this gives rise to a dipole–dipole interaction between the particles. In addition, the energy shift in second-order perturbation theory reduces to

$$E^{(2)}(\{\mathbf{r}_i\}) = \sum_{k\neq i,k\neq j}\frac{|M|^2}{\sqrt{\Delta^2+\Omega^2}}D^2 v(\mathbf{r}_{ik})\,v\big(\mathbf{r}_{jk}\big) + \sum_{i<j}\frac{|N|^2}{2\sqrt{\Delta^2+\Omega^2}}\big[D v\big(\mathbf{r}_{ij}\big)\big]^2$$

and corresponds to a correction to the two-particle interaction potential and a further three-body interaction. The matrix elements M and N take the form

$$M=\alpha\beta\big[\big(\alpha^2\eta_g+\beta^2\eta_e\big)\big(\eta_e-\eta_g\big)+(\alpha^2-\beta^2)/2\big],$$

$$N=\alpha^2\beta^2\big[(\eta_e-\eta_g)^2+1\big].$$

A comparison of the energy shifts $E^{(1)}(\{\mathbf{r}_i\})+E^{(2)}(\{\mathbf{r}_i\})$ with the interaction potential $V_{\rm eff}(\{\mathbf{r}_i\})$ in equation (1) provides the two-particle interaction potential, equation (3), and the three-body interaction in equation (4). The dimensionless coupling parameters take the form $\lambda_1=(\alpha^2\eta_g+\beta^2\eta_e)^2-\alpha^2\beta^2$, $\lambda_2=2|M|^2+|N|^2/2$, and $\gamma_2=2|M|^2$. Note that an n-body interaction term ($n\geq 4$) appears in $(n-1)$th-order perturbation theory in the small parameter $(R_0/a)^3$. Therefore, the contribution of these terms is suppressed and can be safely ignored in our context. Furthermore, the above analysis for $|G\rangle=\Pi_i|+\rangle$ ($\Delta>0$) provides a positive energy shift in second-order $E^{(2)}(\{\mathbf{r}_i\})$, as $|G\rangle$ corresponds to the highest energy state, and provides a repulsive interaction with $\lambda_2\geq 0$ and $\gamma_2\geq 0$. In turn, in an analogous analysis for the lowest energy state, $\Pi_i|-\rangle$, $E^{(2)}$ is negative, which yields a change of sign of the coupling parameters λ_2 and γ_2.

DEGENERATE STATES

For a set-up with $|e_+\rangle_i$ and $|e_-\rangle_i$ degenerate, it is necessary to keep the three states $|+\rangle_i$, $|+\rangle_i$ and $|e_-\rangle_i$ for the perturbative calculation of the Born–Oppenheimer potentials. The leading contribution $E_1(\{\mathbf{r}_i\})$ is not modified, whereas the following term in the dipole–dipole interaction provides a non-vanishing contribution in second-order perturbation theory,

$$\Delta H^{\rm ex}_{\rm d}=\frac{1}{2}\sum_{i\neq j}\frac{D}{2}\Big[\big[\mu(\mathbf{r}_{ij})\big]^* T_i^+S_j^-+\mu(\mathbf{r}_{ij})\,T_i^-S_j^+\Big],$$

with the operators $T_i^+=|e_-\rangle\langle g|$ and $T_i^-=|g\rangle\langle e_-|$ coupling the ground state with the excited state and the potential $\mu(\mathbf{r})=-3(x-iy)^2/r^5$. We therefore obtain a correction to the two-body interaction potential

$$\Delta V(\mathbf{r})=\lambda_3 D R_0^3|\mu(\mathbf{r})|^2,$$

and the three-body interaction

$$W(\mathbf{r}_1,\mathbf{r}_2,\mathbf{r}_3)=\gamma_3\frac{DR_0^3}{2}\sum_{i\neq j\neq k}^{3}[\mu(\mathbf{r}_{ik})]^*\mu(\mathbf{r}_{jk}).$$

The dimensionless parameters λ_3 and γ_3 take the form

$$\lambda_3=\beta^4\alpha^2\frac{\sqrt{\Omega^2+\Delta^2}}{\Delta+3\sqrt{\Omega^2+\Delta^2}}+\alpha^4\beta^2\frac{\sqrt{\Omega^2+\Delta^2}}{\Delta+\sqrt{\Delta^2+\Omega^2}},$$

$$\gamma_3=\alpha^4\beta^2\frac{\sqrt{\Omega^2+\Delta^2}}{\Delta+\sqrt{\Delta^2+\Omega^2}},$$

and depend on the external fields Ed/B and Ω/Δ.

BOSONIZATION

Using the equivalence between hard-core bosons and a spin-1/2 systems allows us to map the hamiltonian in equation (7) to a fermionic model with Fermi operators c_i ($c_i^\dagger$) via a Jordan–Wigner transformation. Following the standard bosonization procedure, we express the fermionic operators via slowly varying left- and right-moving fields[29,30]

$$c_i\sim\sqrt{a}\big[\mathrm{e}^{-ik_{\rm F}x_i}R(x)+\mathrm{e}^{ik_{\rm F}x_i}L(x)\big],$$

where $k_{\rm F}=\pi n/a$ is the Fermi momentum and n is the averaged particle density. Here, x_i describes the position of the lattice site i, whereas a denotes the lattice spacing. The fields $R(x)$ and $L(x)$ are slowly varying and smooth on distances a in the continuous variable $x\sim x_i$ with

$$R(x)=\frac{1}{\sqrt{2\pi a}}\exp\Big(i\sqrt{4\pi}\phi\Big),$$

$$L(x)=\frac{1}{\sqrt{2\pi a}}\exp\Big(-i\sqrt{4\pi}\bar{\phi}\Big).$$

Then, the hamiltonian for non-interacting fermions maps to the Luttinger liquid hamiltonian

$$H_0=\frac{v_{\rm F}\hbar}{2}\int\mathrm{d}x\big[\Pi^2+(\partial_x\Phi)^2\big],$$

with the bosonic field $\Phi=\phi+\bar{\phi}$ and Π the momentum conjugate satisfying the canonical commutation relation $[\Phi(x),\Pi(x')]=i\delta(x-x')$. Here, $v_{\rm F}=2J\sin(\pi n)/\hbar$ denotes the Fermi velocity of the non-interacting Fermi system. To study the influence of the three-body interaction, we split the density

operator, n_i, into its mean value and the fluctuations, that is, $n_i = n + \Delta n_i$. Then, the interaction hamiltonian reduces to $H_{\rm int} = H_1 + H_2 + H_3$ with

$$H_2 = Wn \sum_i [2\Delta n_i \Delta n_{i+1} + \Delta n_{i-1} \Delta n_{i+1}],$$

$$H_3 = W \sum_i \Delta n_{i-1} \Delta n_i \Delta n_{i+1},$$

where H_1 denotes a shift in the chemical potential and can be dropped. The density operator expressed in the right- and left-moving fields takes the form

$$\Delta n_i = a\left[\partial_x \Phi + e^{2ik_F x_i} M^+(x) + e^{-2ik_F x_i} M^-(x)\right],$$

with

$$M^+(x) =: R^\dagger(x) L(x) :, \quad M^-(x) =: L^\dagger(x) R(x) : .$$

When expressing the interaction hamiltonian $H_{\rm int}$ in terms of the bosonic fields Φ special care has to be taken owing to the normal ordering $: \ :$ of the operators. Furthermore, we note that some terms exhibit fast oscillations, which can be ignored in the low-energy hamiltonian. Then, the interaction hamiltonian H_2 takes the form

$$H_{\rm int} = Wna \int dx \frac{1}{\pi} [3 - 2\cos(2\pi n) - \cos(4\pi n)] (\partial_x \Phi)^2 .$$

Furthermore, at half filling with $n = 1/2$ a further term appears owing to cancellation of different oscillating terms, which takes the sine-Gordon form

$$H_{\rm sG} = u \int dx \frac{1}{\pi^2 a^2} \cos(\beta \Phi), \qquad (10)$$

with $u = Wna$ and $\beta = \sqrt{16\pi}$. The interaction H_3 only contributes less relevant terms, except at fillings $n = 1/3$ and $n = 2/3$. Then a further term appears, which takes the sine-Gordon form in equation (10) with parameters $u = Wa/\pi$ and $\beta = \sqrt{36\pi}$.

Received 26 March 2007; accepted 27 June 2007; published 22 July 2007.

References

1. Murphy, R. D. & Barker, J. A. Three-body interactions in liquid and solid helium. *Phys. Rev. A* **3**, 1037–1040 (1971).
2. Moore, G. & Read, N. Nonabelions in the fractional quantum Hall effect. *Nucl. Phys. B* **360**, 362–396 (1991).
3. Fradkin, E., Nayak, C., Tsvelik, A. & Wilczek, F. A Chern-Simons effective field theory for the Pfaffian quantum Hall state. *Nucl. Phys. B* **516**, 704–718 (1998).
4. Cooper, N. R. Exact ground states of rotating Bose gases close to a Feshbach resonance. *Phys. Rev. Lett.* **92**, 220405 (2004).
5. Moessner, R. & Sondhi, S. L. Resonating valence bond phase in the triangular lattice quantum dimer model. *Phys. Rev. Lett.* **86**, 1881–1884 (2001).
6. Balents, L., Fisher, M. P. A. & Girvin, S. M. Fractionalization in an easy-axis kagome antiferromagnet. *Phys. Rev. B* **65**, 224412 (2002).
7. Motrunich, O. I. & Senthil, T. Exotic order in simple models of bosonic systems. *Phys. Rev. Lett.* **89**, 277004 (2002).
8. Hermele, M., Fisher, M. P. A. & Balents, L. Pyrochlore photons: The $U(1)$ spin liquid in a $S = 1/2$ three dimensional frustrated magnet. *Phys. Rev. B* **69**, 064404 (2004).
9. Levin, M. A. & Wen, X. G. String-net condensation: A physical mechanism for topological phases. *Phys. Rev. B* **71**, 045110 (2005).
10. Fidkowski, L., Freedman, M., Nayak, C., Walker, K. & Wang, Z. From string nets to nonabelions. Preprint at <http://www.arxiv.org/cond-mat/0610583> (2006).
11. Micheli, A., Brennen, G. K. & Zoller, P. A toolbox for lattice-spin models with polar molecules. *Nature Phys.* **2**, 341–347 (2006).
12. Ronen, S., Bortolotti, D. C. E., Blume, D. & Bohn, J. L. Dipolar Bose–Einstein condensates with dipole-dependent scattering length. *Phys. Rev. A* **74**, 033611 (2006).
13. Kotochigova, S. & Tiesinga, E. Controlling polar molecules in optical lattices. *Phys. Rev. A* **73**, 041405(R) (2006).
14. Baranov, M. A., Osterloh, K. & Lewenstein, M. Fractional quantum Hall states in ultracold rapidly rotating dipolar Fermi gases. *Phys. Rev. Lett.* **94**, 070404 (2005).
15. Wang, D.-W., Lukin, M. D. & Demler, E. Quantum fluids of self-assembled chains of polar molecules. *Phys. Rev. Lett.* **97**, 180413 (2006).
16. Santos, L., Shlyapnikov, G. V. & Lewenstein, M. Roton-maxon spectrum and stability of trapped dipolar Bose–Einstein condensates. *Phys. Rev. Lett.* **90**, 250403 (2003).
17. Doyle, J., Friedrich, B., Krems, R. V. & Masnou-Seeuws, F. Quo vadis, cold molecules? *Eur. Phys. J. D* **31**, 149–164 (2004).
18. Sage, J. M., Sainis, S., Bergeman, T. & DeMille, D. Optical production of ultracold polar molecules. *Phys. Rev. Lett.* **94**, 203001 (2005).
19. Rieger, T., Junglen, T., Rangwala, S. A., Pinkse, P. W. H. & Rempe, G. Continuous loading of an electrostatic trap for polar molecules. *Phys. Rev. Lett.* **95**, 173002 (2005).
20. Wang, D. *et al.* Photoassociative production and trapping of ultracold KRb molecules. *Phys. Rev. Lett.* **93**, 243005 (2005).
21. Mancini, M. W., Telles, G. D., Caires, A. R. L., Bagnato, V. S. & Marcassa, L. G. Observation of ultracold ground-state heteronuclear molecules. *Phys. Rev. Lett.* **92**, 133203 (2004).
22. van de Meerakker, S. Y. T., Smeets, P. H. M., Vanhaecke, N., Jongma, R. T. & Meijer, G. Deceleration and electrostatic trapping of OH radicals. *Phys. Rev. Lett.* **94**, 23004 (2005).
23. Kraft, S. D. *et al.* Formation of ultracold LiCs molecules. *J. Phys. B* **39**, S993–S1000 (2006).
24. Sawyer, B. C. *et al.* Magneto-electrostatic trapping of ground state OH molecules. Preprint at <http://www.arxiv.org/physics/0702146> (2007).
25. Tewari, S., Scarola, V. W., Senthil, T. & Sarma, S. D. Emergence of artificial photons in an optical lattice. *Phys. Rev. Lett.* **97**, 200401 (2006).
26. Micheli, A., Pupillo, G., Büchler, H. P. & Zoller, P. Cold polar molecules in 2d traps: Tailoring interactions with external fields for novel quantum phases. Preprint at <http://www.arxiv.org/quant-ph/0703031> (2007).
27. Büchler, H. P. *et al.* Strongly correlated 2D quantum phases with cold polar molecules: Controlling the shape of the interaction potential. *Phys. Rev. Lett.* **98**, 060404 (2007).
28. Jaksch, D., Bruder, C., Cirac, J. I., Gardiner, C. W. & Zoller, P. Cold bosonic atoms in optical lattices. *Phys. Rev. Lett.* **81**, 3108–3111 (1998).
29. Gogolin, A. O., Nersesyan, A. A. & Tsvelik, A. M. *Bosonization and Strongly Correlated Systems* (Cambridge Univ. Press, Cambridge, 1998).
30. Sachdev, S. *Quantum Phase Transitions* (Cambridge Univ. Press, Cambridge, 1999).
31. Haldane, F. D. M. Effective harmonic-fluid approach to low energy properties of one-dimensional quantum fluids. *Phys. Rev. Lett.* **47**, 1840–1843 (1981).

Acknowledgements

We would like to thank M. Lukin and A. Gorshkov for discussions. This work was supported by the Austrian Science Foundation (FWF), the European Union projects OLAQUI (FP6-013501-OLAQUI), CONQUEST (MRTN-CT-2003-505089), the SCALA network (IST- 15714), the Institute for Quantum Information, and in part by the National Science Foundation under Grant No. PHY05-51164. Correspondence and requests for materials should be addressed to H.P.B.

Competing financial interests

The authors declare no competing financial interests.